

ICESat profiles of tabular iceberg margins and iceberg breakup at low latitudes

Ted Scambos,¹ Olga Sergienko,² Aitbala Sargent,³ Douglas MacAyeal,² and Jim Fastook³

Received 14 June 2005; revised 18 September 2005; accepted 10 October 2005; published 3 November 2005.

[1] ICESat elevation profiles of tabular iceberg margins and the Ronne Ice Shelf edge reveal shapes indicative of two types of bending forces. Icebergs and shelf fronts in sea-ice-covered areas have broad (~ 1000 m wide), rounded, ~ 0.6 m high ‘berms’ and outer edges that slope down several meters toward the water. Berms in warmer water have 2 to 5 m ‘ramparts’ with ~ 1500 m wide edge-parallel ‘moats’ inboard of the edge. This latter pattern was first revealed in images from International Space Station (ISS) showing edge-parallel melt ponds on one iceberg just prior to its disintegration. Model results indicate the patterns are caused by hydrostatic and lithostatic forces acting on the ice face. ‘Berm’ profiles arise from differences between ice and water pressure along the face. ‘Rampart-moat’ profiles result from waterline erosion, creating a submerged bench of ice that lifts the ice edge. We use the results to discuss iceberg breakup at low latitudes. **Citation:** Scambos, T., O. Sergienko, A. Sargent, D. MacAyeal, and J. Fastook (2005), ICESat profiles of tabular iceberg margins and iceberg breakup at low latitudes, *Geophys. Res. Lett.*, *32*, L23S09, doi:10.1029/2005GL023802.

1. Introduction

[2] Large tabular icebergs have physical characteristics and stress environments similar to ice shelves, but with an important difference: they drift. Therefore they can experience more rapid changes in climate and ocean temperature than ice shelves, and can be used as a proxy to investigate how ice shelves respond to climate change. Here we examine several changes that occur during iceberg drift using the Ice, Cloud and land Elevation Satellite (ICESat). ICESat carries a single instrument, the Geoscience Laser Altimeter System (GLAS). The system gathers elevation data from a ~ 70 m ground spot (‘shot’) every 172 ± 3 m [Zwally *et al.*, 2002]. Vertical precision under ideal conditions, e.g. dry lake beds, is 4 cm [Fricker *et al.*, 2005]. ICESat’s global coverage, precision, and high along-track resolution opens new research avenues for studying the evolution and melt rate of these large freshwater ice masses.

[3] In late 1998 and early 2000, three large icebergs calved from the Ronne Ice Shelf [Lazzara *et al.*, 1999]. Initially designated A38, A43, and A44, these bergs calved

into smaller pieces (indicated by suffix letters; see the National Ice Center, www.natice.gov, for naming conventions) and drifted north along similar paths (Figure 1). This pattern of drift has been observed many times [e.g., *Swithinbank et al.*, 1977], and was even exploited (unknowingly, perhaps) by Shackleton and his companions aboard the *James Caird* in 1915 on the *Endurance* expedition.

2. ICESat Observations and Data Analysis

[4] Elevations from the Global Elevation Data product (GLA06; Release 18) were used from six operations periods beginning in February 2003 (Laser 1 to Laser 3a) [see *Schutz et al.*, 2005]. A total of 19 elevation profiles from icebergs A38A, A38B, A43A, A43B and A43F, and the Ronne Ice Shelf front at the A43 calving site, were examined. Shot point location accuracy was no worse than ± 200 m for all operation periods. Shot-to-shot elevation variations (a measure of accuracy and the effects of surface roughness) were determined by subtracting the mean shelf and iceberg surface slope from the profile values. The RMS of the variation is ± 10 cm.

[5] ICESat tracks cross the iceberg edges at random orientations due to drift. To compare the tracks with each other and with simplified models, the profiles were re-projected to a line perpendicular to the berg margin. Using near-coincident images of the icebergs from the Moderate-resolution Imaging Spectro-radiometer (MODIS; Band 1 with 250 m resolution), the approximate angle ($\pm 3^\circ$) between the berg margin and the ICESat track was determined, and shot-to-shot separation for the profile was multiplied by the sine of that angle. Profiles intersecting the edge at $\leq 30^\circ$ were not considered, nor were profiles near iceberg ‘corners’ (acute angles in the perimeter shape on a ~ 3 km scale). In general, there was little evidence of drift in the interval between ICESat and MODIS data; however, for bergs in the Scotia Sea, offsets of up to 14 km were seen in just a few hours. True profile position on the berg could be estimated in these cases because iceberg motion was mostly translational.

[6] Distance from the margin is referenced to the midpoint between the two sequential ICESat ‘shots’ that record the ocean surface (or sea ice) and the surface of the iceberg, respectively. Freeboard elevation in sea ice areas is referenced to the lowest geoid elevation within 2 km of the berg face, or, for open ocean, the mean ocean elevation within 2 km of the berg. This removes potential geoid errors, tide errors, and systematic errors between profiles to a precision of about 30 cm.

[7] The ‘berm’ and ‘rampart-moat’ profiles show variations of scale, but shape type is consistently associated with the iceberg’s latitude and presence of sea ice cover

¹National Snow and Ice Data Center, University of Colorado, Boulder, Colorado, USA.

²Department of Geophysical Sciences, University of Chicago, Chicago, Illinois, USA.

³Quaternary Institute and Computer Sciences Department, University of Maine, Orono, Maine, USA.

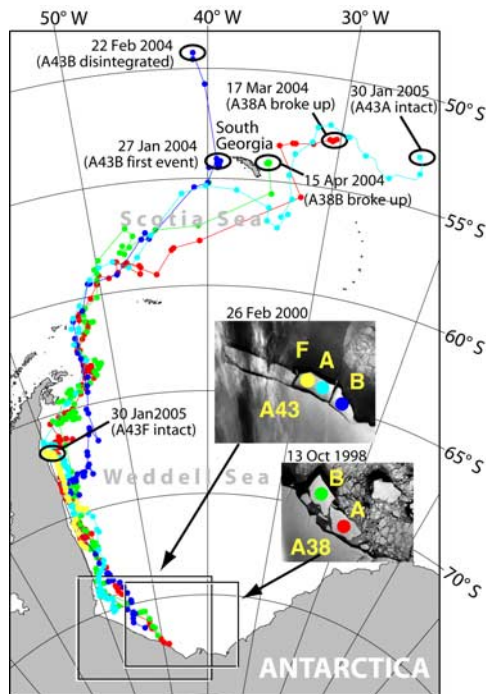


Figure 1. Iceberg drift tracks for the five Ronne Ice Shelf-derived icebergs studied. Berg locations are plotted every ~ 10 days. Insets are satellite images of the shelf front soon after the initial calving events.

(Figure 2). The Ronne Ice Shelf front and all icebergs within sea ice (south of $\sim 63^\circ\text{S}$), showed berm-type profiles, having ~ 0.6 m raised rounded berms with maximum height at about 2 ice thicknesses from the shelf/berg edge. (Shelf and iceberg thicknesses are estimated from elevation using the relationship given by *Bamber and Bentley* [1994].) From this crest to the ice margin, ‘berm’ profiles have relatively steep slopes (0.009–0.011) dipping 2 to 3 m towards the sea surface. Similar profiles were observed on rifts in the Ross and Amery Ice Shelves (H. Fricker et al., ICESat’s new perspective on ice shelf rifts: The vertical dimension, submitted to *Geophysical Research Letters*, 2005). Icebergs north of the sea ice edge have a consistent pattern of raised edges (‘ramparts’) with shallow (50 to 100 cm deep) ‘moat’ areas inboard and parallel to the margin. The lowest point of the ‘moat’ is 3 to 4 ice thicknesses from the ice edge. In one profile, a berg within very open pack ice near the sea ice margin has a subdued ‘berm’ profile, perhaps indicating a transitional shape.

[8] Consecutive profiles crossing the same iceberg showed freeboard elevation changes of up to 5 meters (Table 1). Since profiles cross the bergs at random orientations, and the bergs drift and rotate between profiles, elevation comparisons required aligning the berg shapes and their projected elevation data by rotating MODIS image sub-scenes to match the iceberg outlines. Elevation changes were small but significant for bergs south of the sea ice edge, and larger for bergs in the Scotia Sea or near South Georgia. Both firm densification and basal melting may contribute to elevation changes. However, basal melting likely accounts for most of the change in the austral winter period (e.g., A43A in 2003). Basal melting was proposed as

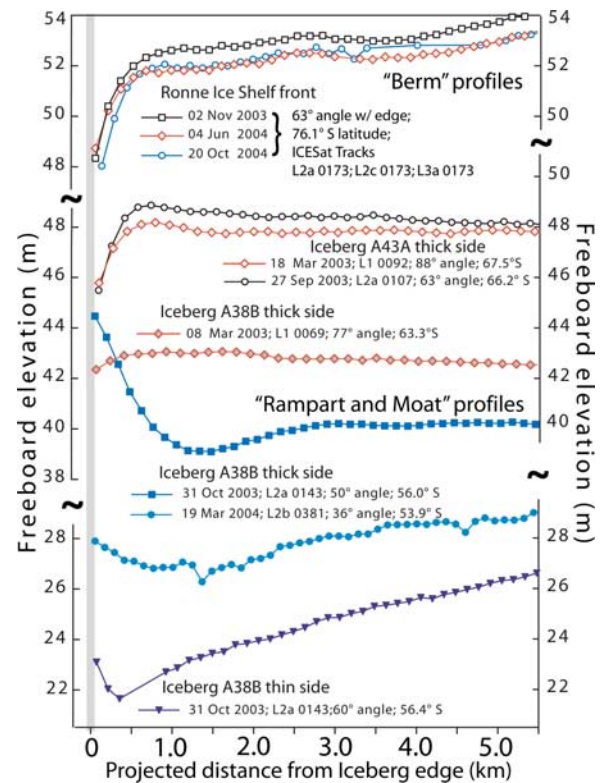


Figure 2. Examples of ICESat elevation profiles over iceberg and ice shelf margins. Open symbols indicate the shelf or berg front was in sea ice; solid symbols indicate the iceberg was in open water; gray-fill symbols (A38B, 08 March 2003) indicate partial sea ice cover.

an explanation for elevation trends of the Larsen B and C ice shelves [*Shepherd et al.*, 2003].

3. MODIS and ISS Images

[9] Additional MODIS images, some using true-color band combinations, record changes in the icebergs during drift (Figures 3 and 4). True color images facilitate an assessment of melt pond extent on the bergs, and help identify thin clouds or shadows. In addition, A43B was photographed by astronauts aboard ISS in January, 2004, revealing extensive melt ponds, some impounded by edge-parallel moats. The photographs initiated this study.

[10] The images record three patterns of iceberg breakup: ‘edge-wasting’, where small (<10 km²), edge-parallel calvings reduce the iceberg’s area without greatly changing its

Table 1. Freeboard Elevation Changes in Drifting Icebergs From ICESat Profiles

Iceberg	Date (Location)	Elevation, m
A38B	08 Mar 2003 (63.3°S) to 19 Mar 2004 (53.9°S)	31.5 ± 0.5 to 26.5 ± 0.5
A38A	21 Feb 2003 (62.7°S) to 31 Oct 2003 (58.0°S)	36.5 ± 0.3 to 34.5 ± 0.5
A43A ^a	18 Mar 2003 (67.5°S) to 27 Sep 2003 (66.1°S)	48.3 ± 0.2 to 47.5 ± 0.2
A43A ^a	18 Mar 2003 (67.5°S) to 15 Mar 2004 (63.6°S)	47.8 ± 0.2 to 46.7 ± 0.2

^aProfile intersections are not over the same point on the iceberg.

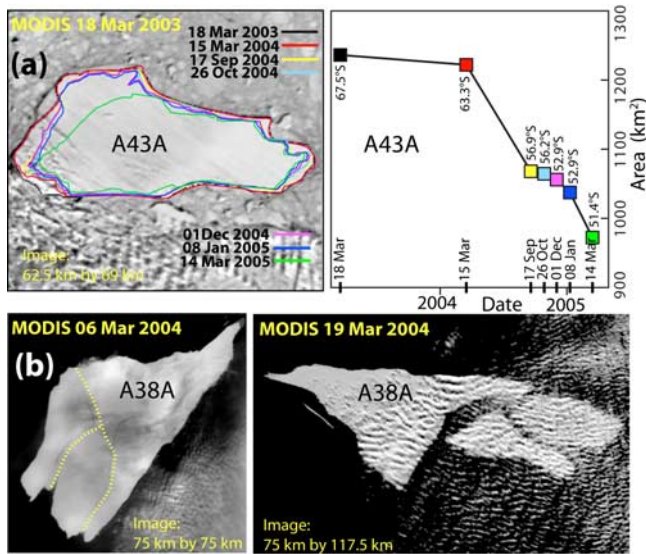


Figure 3. Two breakup patterns of icebergs. (a) Edge-wasting, A43A: upper left, MODIS image with iceberg outlines from later images; upper right, iceberg area versus time, with latitude at time of measurement. (b) Large-scale calving, A38A: lower left, dotted lines are parallel to pre-existing rifts that controlled calving; lower right, after calving.

shape (Figure 3a); major calvings, where bergs break into a few large pieces (Figure 3b); and disintegration, in which a melt-water-flooded iceberg rapidly calves a large number of small (sub-resolution) icebergs (Figure 4). These patterns are analogous to calving styles of ice shelves, e.g., margin ‘spalling’ events, large iceberg calvings, and ice shelf disintegration, as with the Larsen B breakup in 2002 [Scambos *et al.*, 2003]. Iceberg edge-wasting increases rapidly as the bergs drift north of the sea ice edge into the Scotia Sea (Figure 3a). There is a continuum of calving scales between edge wasting and major calvings, but major calvings often follow pre-existing rifts rather than the

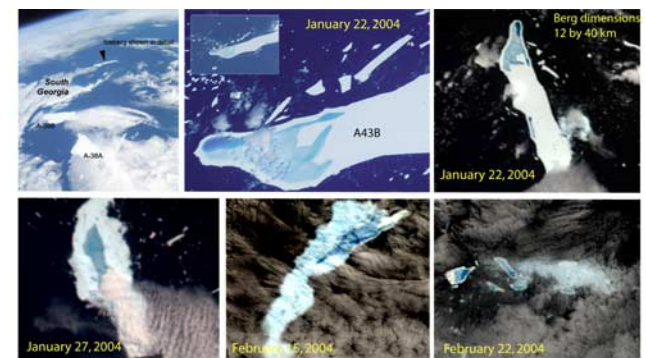


Figure 4. The disintegration of iceberg A43B. Upper left, photograph from ISS show orbital view of three icebergs surrounding South Georgia island (ISS008-E-12564). Upper center, melt ponds on A43B tend to align a few hundred meters inboard of the ice edge (ISS008-E-12555). Upper right and bottom row, MODIS true-color images of A43B record its disintegration over the following month.

iceberg edge (Figure 3b). Major calvings occur in all seasons and areas: A43A calved the A43F iceberg in June, 2001 at 71.8°S; both A38A and A38B broke into a few large pieces in March/April of 2004, near 54°S. Only A43B showed the disintegration pattern (Figure 4); it was also the only iceberg with surface melt ponds.

4. Forces at an Iceberg Face, and Modeling

[11] Past studies have investigated ice shelf edge structure [Reeh, 1968; Fastook, 1984], and the effect of torques acting on an iceberg or shelf edge (Figure 5), but the ‘rampart-moat’ profile has not been previously observed or modeled. ‘Berm’ profiles arise from the difference in pressure gradient between water and ice along the vertical face of floating ice. Because water pressure increases faster with depth than ice lithostatic pressure, there is a net torque in the direction of rotating the top edge outward and down toward the water. A second force we consider is the buoyancy of a submerged ‘bench’ of ice. We infer that rapid waterline erosion of an iceberg leads to this shape [Hughes, 2002].

[12] We use two models, and review the results of Reeh [1968], to investigate the ‘berm’ pattern (Figure 6, top). Model investigations are exploratory, and do not include ice density or temperature variations, or face orientations other than vertical. An elastic plate bending approach [Sergienko *et al.*, 2004], using the full estimated ice thickness and a standard value for Young’s modulus (e_{ice} , 8.88 Mpa @ $-5^{\circ}C$), leads to berm amplitudes and wavelengths that are too large by a factor of ~ 4 relative to the observed profiles (not shown in Figure 6). By adjusting e downward significantly ($0.3 e_{ice}$), and reducing the thickness, we approach a profile similar to those observed (‘Elastic model’ in Figure 6); clearly plastic deformation effects are important. In another model, modified from Fastook [1984], two-dimensional stress balance equations incorporating Glen’s flow law and using ice strength parameters for $-12^{\circ}C$ mean temperature, are solved using a finite element model (‘FEM’ in Figure 6). Reeh [1968] considers the viscous deformation of a floating ice plate over time. Using his graphical solutions, the ‘berm’ profiles are best approximated using a mean ice temperature of $-12^{\circ}C$, a firm-corrected ice thickness value of 300 to 350 m, and a time factor (time since last calving) of ~ 1.5 years (‘Viscous model’ in Figure 6). A

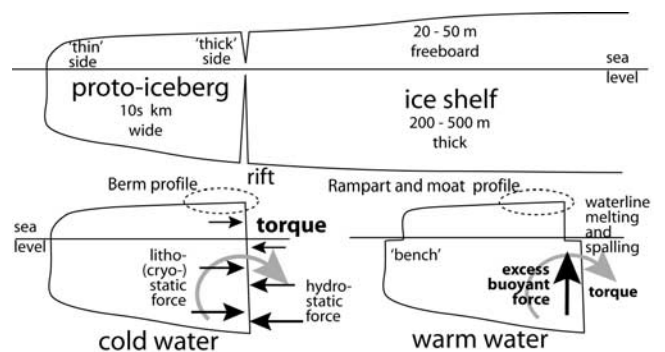


Figure 5. Schematic cross-sections of ice shelf and icebergs, illustrating basic characteristics, nomenclature, and the physical basis for our model experiments.

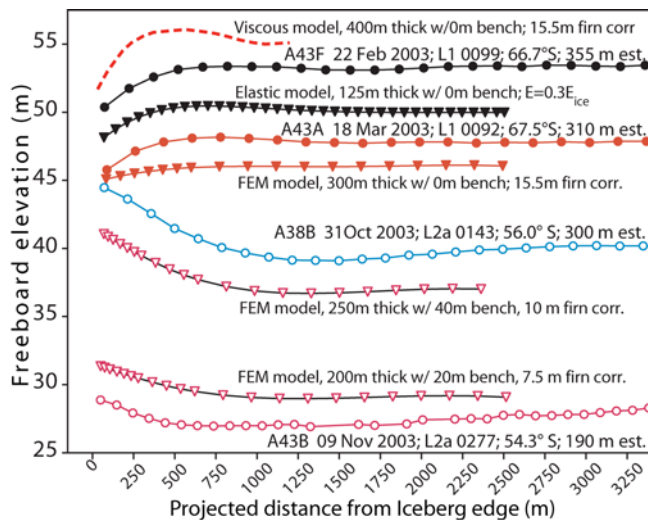


Figure 6. Comparison of ICESat observed profiles and selected model runs. Viscous model profile is from Reeh [1968, Figure 6]. ICESat profiles used in setting model parameters are shown with ancillary information similar to Figure 2.

shorter time since calving, and colder mean temperature, might have more closely matched the profiles, but these were not explicitly covered by Reeh [1968].

[13] For the ‘rampart-moat’ case, we examine the effects of an ice bench of varying widths with an upper surface 5m below water level using the finite element model. Benches of just a few meters width were sufficient to completely eliminate the ‘berm’ shape and lift the iceberg margin higher than the mean freeboard. We find that benches of 20 to 40 meters width best match the observed warm-water berg profiles. (Ice thickness estimates for model comparisons to the warm-climate icebergs assume a modified firm density due to warming, melt, rain, etc.; Figure 6, bottom).

5. Hypothetical Scenarios for Iceberg Evolution and Breakup

[14] The profiles, images, and model results, coupled with past studies of the relationship between surface melt ponds and ice shelf disintegration, suggest that iceberg break up in above-freezing air and water may be controlled by the marginal stress pattern of the ice. We infer that growth of the ice bench is limited by bottom fracturing induced by the buoyancy, and that cyclical bench formation and calving may account for some of the ‘edge-wasting’ berg events. Initially after a calving, it is assumed that the ice would have a ‘berm’ profile, until waterline melting and erosion produced an ice bench and an uplifted rampart.

[15] Stresses and fracturing related to the two profile types may be a key factor in the pattern of breakup. Under dry conditions, stresses great enough to initiate crevassing at a berm crest or foreslope may not lead to a calving event; so breakup may be controlled by ‘edge-wasting’ and tidally-driven berg flexure leading to major calving events. However, once surface ponding occurs, it is possible that a runaway fragmentation of the iceberg would ensue upon the loss of the bench and rampart, due to melt-water enhanced fracturing [e.g., Scambos *et al.*, 2003]. We plan further investigations of both icebergs and ice shelf edges using ICESat.

[16] **Acknowledgments.** We thank NASA’s ICESat Science Project and the NSIDC for distribution of ICESat data, see <http://icesat.gsfc.nasa.gov> and <http://nsidc.org/data/icesat>. David Long and the National Ice Center provided iceberg locations. ISS images were provided by the Image Analysis Laboratory, NASA Johnson Space Center. This work was funded by NASA Snow and Ice DAAC contract NAS5-03099 and by NSF-OPP grant 0337165.

References

- Bamber, J., and C. Bentley (1994), Comparison of satellite-altimetry and ice-thickness measurements of the Ross Ice Shelf, Antarctica, *Ann. Glaciol.*, **20**, 357–364.
- Fastook, J. (1984), Ice shelves and ice streams: Three modeling experiments, in *Glaciers, Ice Sheets, and Sea Level: Effect of a CO₂-Induced Climatic Change*, U.S. Dep. of Energy Rep. DOE/CV/60235-1, pp. 279–300, Washington, D. C.
- Fricke, H. A., A. Borsa, B. Minster, C. Carabajal, K. Quinn, and B. Bills (2005), Assessment of ICESat performance at the salar de Uyuni, Bolivia, *Geophys. Res. Lett.*, **32**, L21S06, doi:10.1029/2005GL023423.
- Hughes, T. (2002), Calving bays, *Quat. Sci. Rev.*, **7**, 267–282.
- Lazzara, M., K. Jezek, T. Scambos, D. MacAyeal, and C. van der Veen (1999), On the recent calving of icebergs from the Ross Ice Shelf, *Polar Geogr.*, **23**, 201–212.
- Reeh, N. (1968), On the calving of ice from floating glaciers and ice shelves, *J. Glaciol.*, **7**, 215–232.
- Scambos, T., C. Hulbe, and M. Fahnestock (2003), Climate-induced ice shelf disintegration in the Antarctic Peninsula, in *Antarctic Peninsula Climate Variability: Historical and Paleoenvironmental Perspectives*, *Antarct. Res. Ser.*, vol. 79, edited by E. Domack *et al.*, pp. 79–92, AGU, Washington, D. C.
- Schutz, B. E., H. J. Zwally, C. A. Shuman, D. Hancock, and J. P. DiMarzio (2005), Overview of the ICESat Mission, *Geophys. Res. Lett.*, **32**, L21S01, doi:10.1029/2005GL024009.
- Sergienko, O., T. Scambos, D. MacAyeal, and J. Fastook (2004), Tabular icebergs in the South Atlantic: Melt ponding, melt pond geometry, and margin evolution, *Eos Trans. AGU*, **85**(47), C22A-07.
- Shepherd, A., D. Wingham, T. Payne, and P. Skvarca (2003), Larsen Ice Shelf has progressively thinned, *Science*, **302**, 856–859.
- Swifthbank, C., P. McClain, and P. Little (1977), Drift tracks of Antarctic icebergs, *Polar Rec.*, **18**, 495–500.
- Zwally, H. J., *et al.* (2002), ICESat’s laser measurements of polar ice, atmosphere, ocean, and land, *J. Geodyn.*, **34**, 405–445.

J. Fastook and A. Sargent, Quaternary Institute, University of Maine, Orono, ME 04469, USA.

D. MacAyeal and O. Sergienko, Department of Geophysical Sciences, University of Chicago, Chicago, IL 60637, USA.

T. Scambos, National Snow and Ice Data Center, University of Colorado, Boulder, CO 80309–0449, USA. (teds@icehouse.colorado.edu)